Electronic Supplementary Material (ESI) for Journal of Materials Chemistry A.

Highly reversible aluminium-sulfur batteries through effective sulfur confinement with hierarchical porous carbon

Dian Zhang,[a†] Xu Zhang,[a†] Boya Wang,[a] Shiman He,[a] Shiqi Liu,[a] Mingxue Tang[b] and Haijun Yu[a*]

[a]College of Materials Science and Engineering, Faculty of Materials and Manufacturing, Beijing University of Technology, Beijing, 100124, China. E-mail: hj-yu@bjut.edu.cn

[b]Center for High Pressure Science & Technology Advanced Research, Beijing 100094, China.

[†]The two authors contributed equally to this work.

*Corresponding author. E-mail: hj-yu@bjut.edu.cn

Figure S1. An optical image of the viscous solution containing the N-rich polymer precursor and well-disolved $Zn(NO_3)_2 \cdot 6H_2O$ for preparing HPCK.

Figure S2. An optical image of HPC.

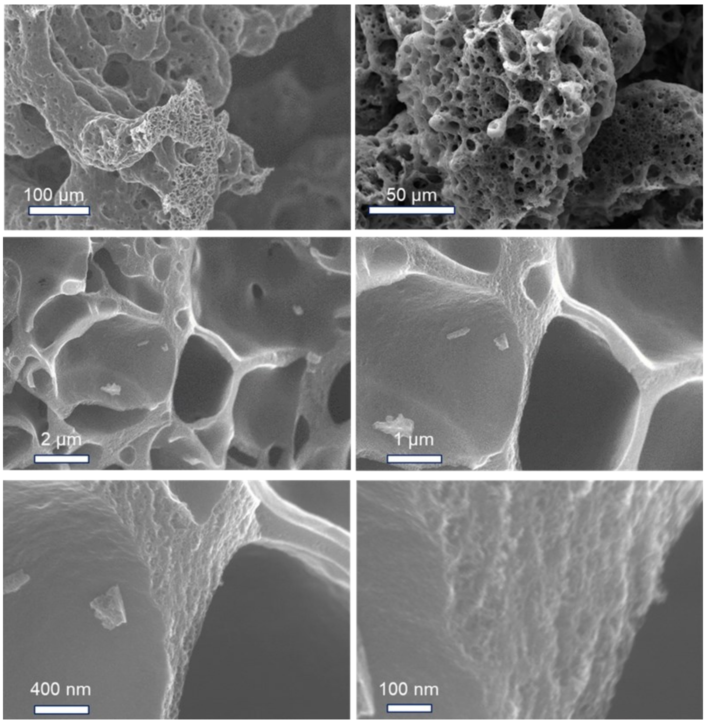

Figure S3. SEM images of HPC.

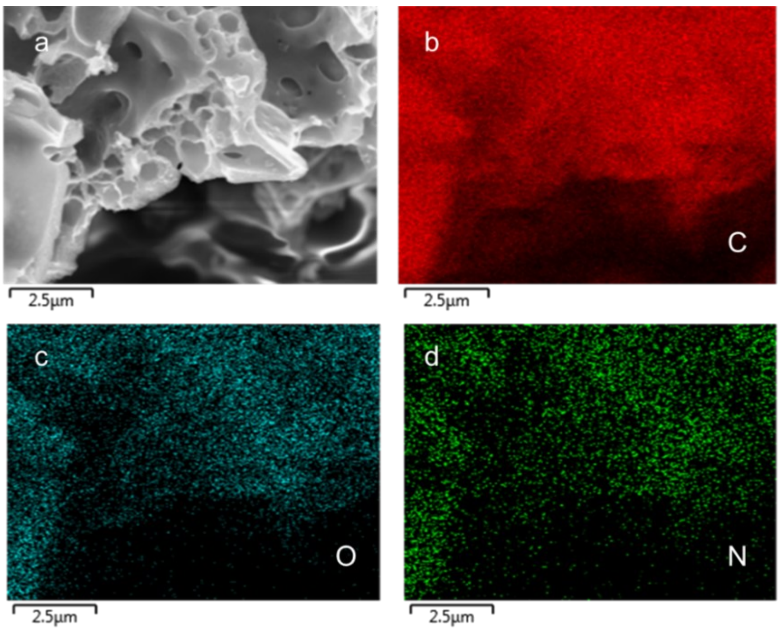

Figure S4. (a) SEM image of HPCK and its EDS mapping images of (b) C, (c) O and (d) N.

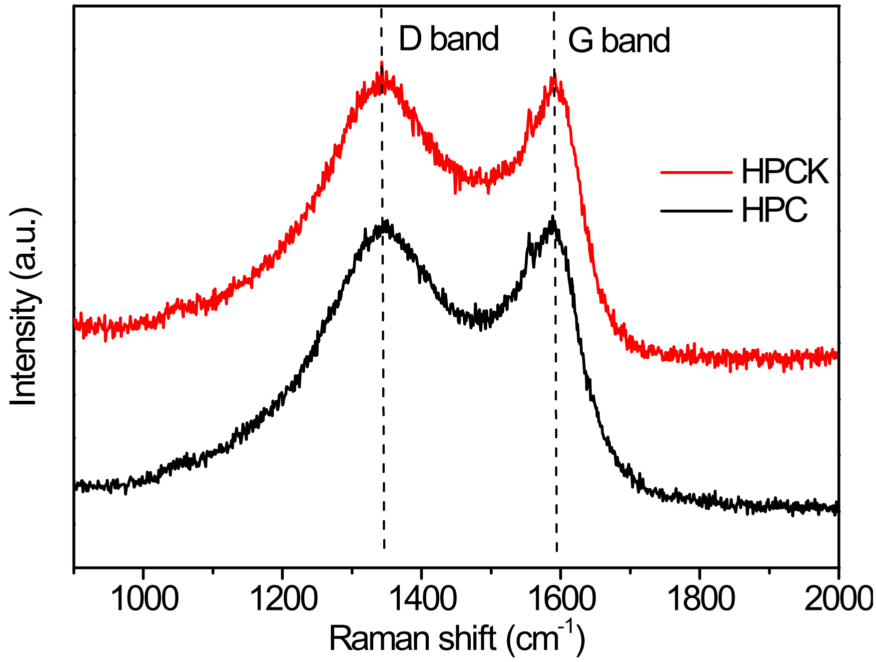

Figure S5. Raman spectra of HPC and HPCK.

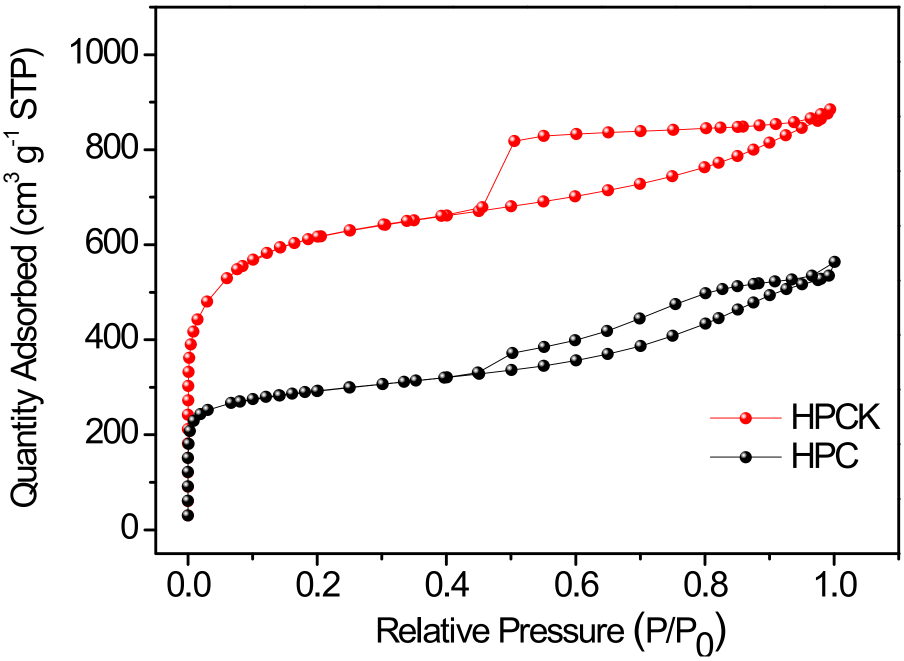

Figure S6. Nitrogen adsorption-desorption isotherms of HPC and HPCK.

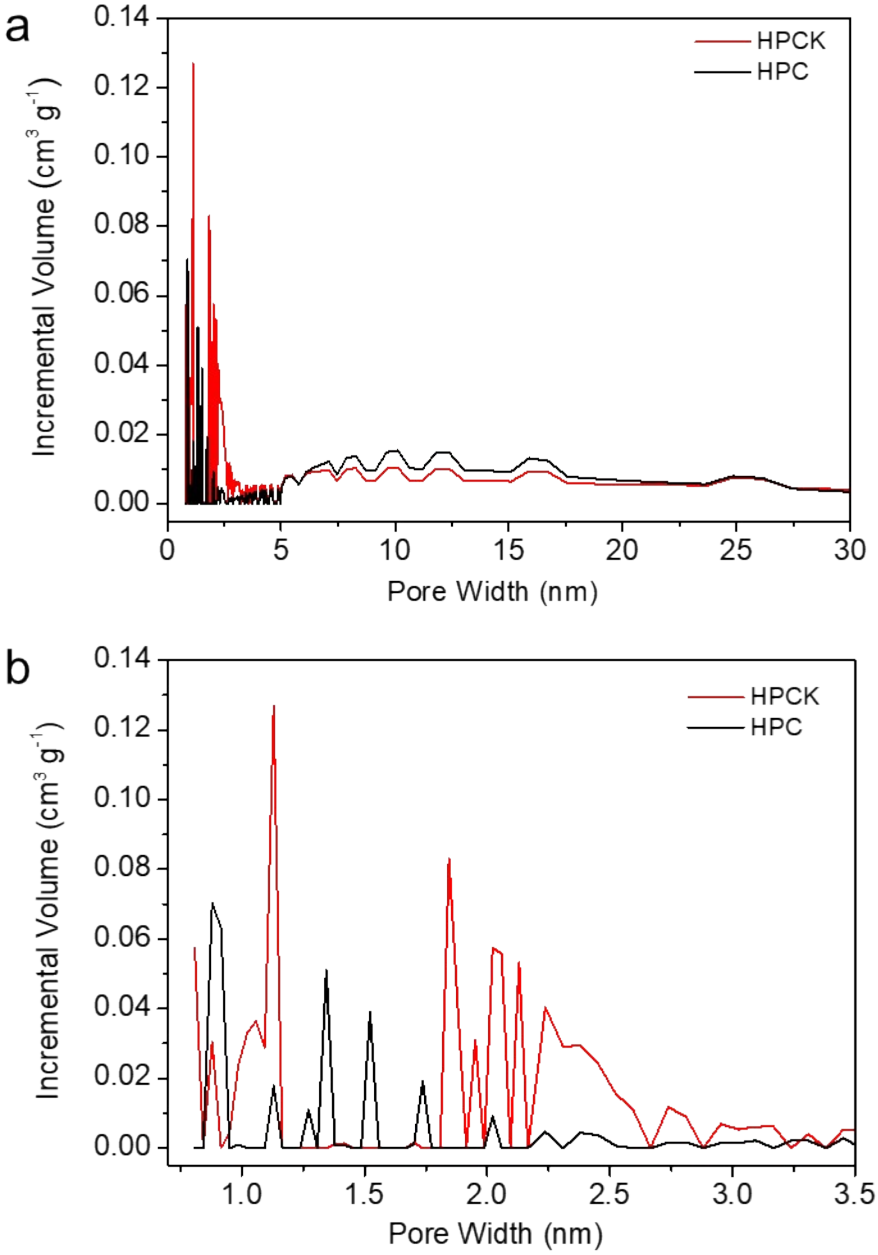

Figure S7. Porous distributions of HPC and HPCK. The range of pore width is 0 ~ 30 nm (a) and 0.6 ~ 3 nm (b).

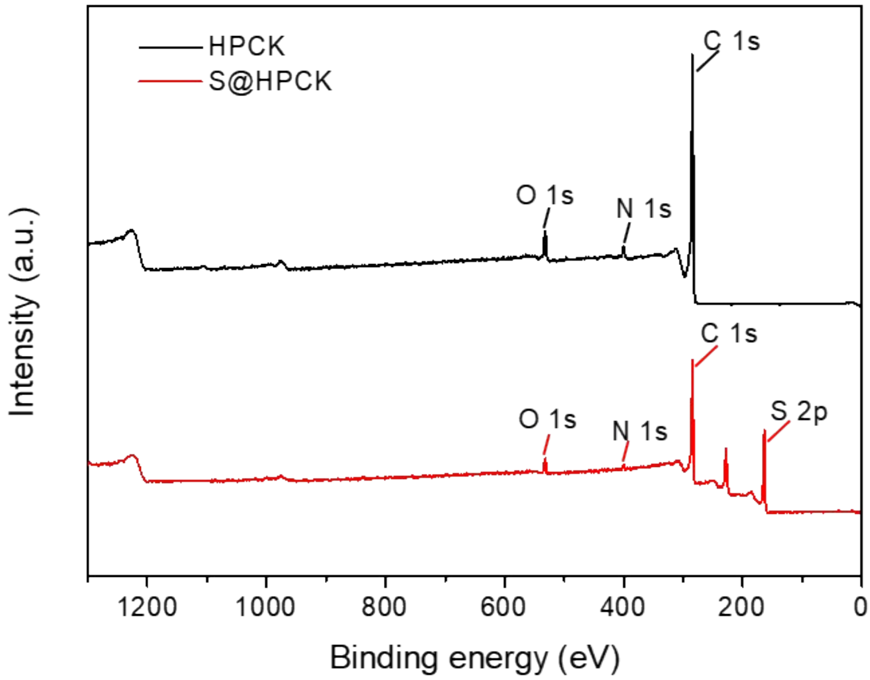

Figure S8. XPS survey spectra of HPCK and S@HPCK.

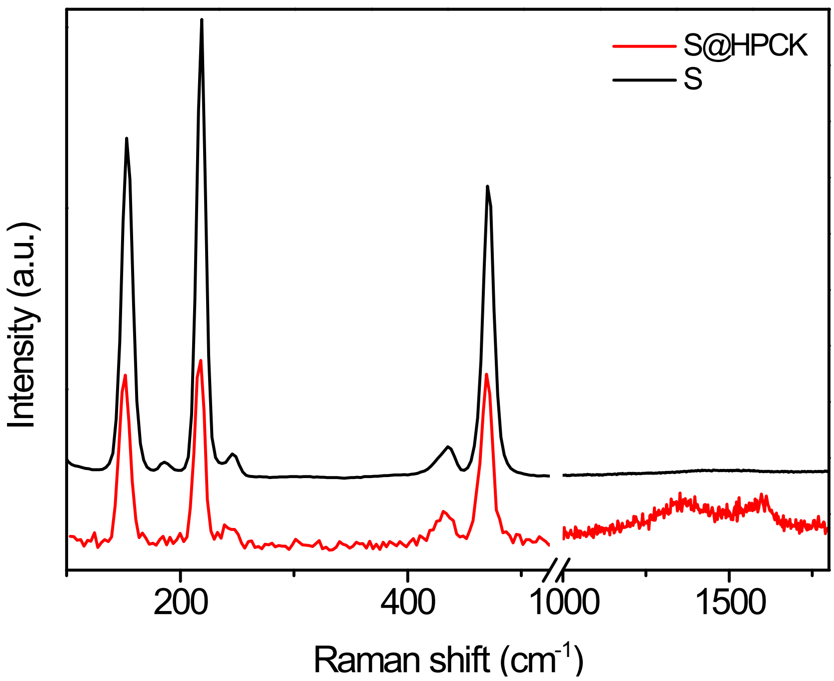

Figure S9. Raman spectra of S and S@HPCK.

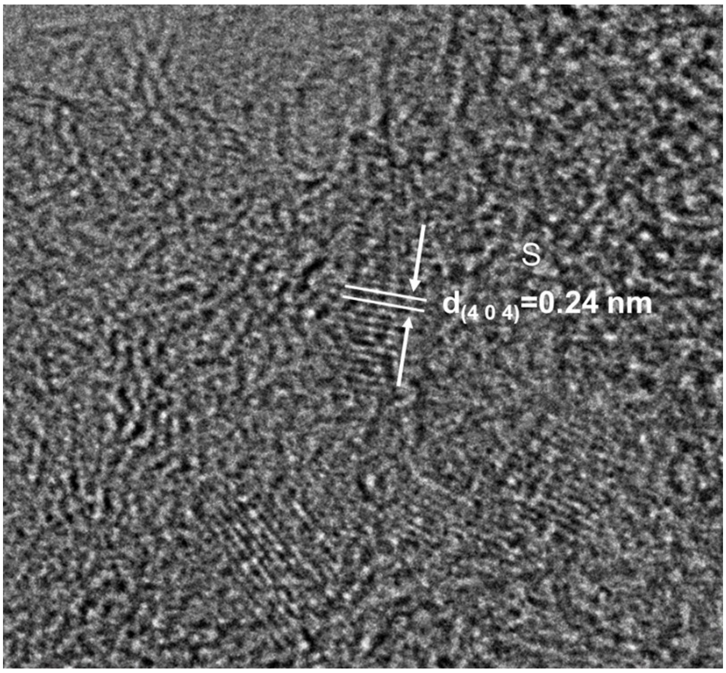

Figure S10. TEM image of S@HPCK showing the lattice of S surrounded by HPCK.

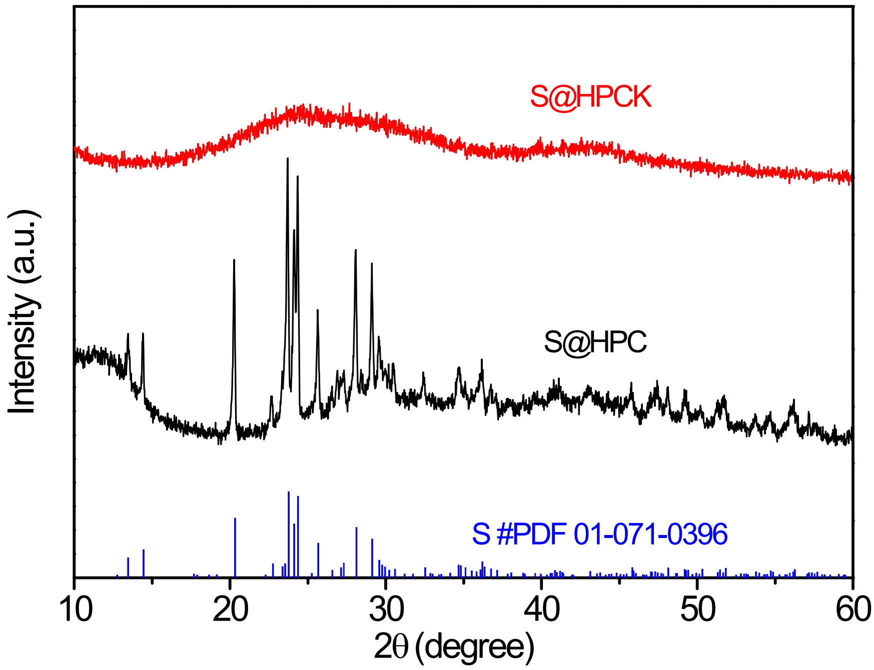

Figure S11. XRD patterns of S, S@HPC and S@HPCK.

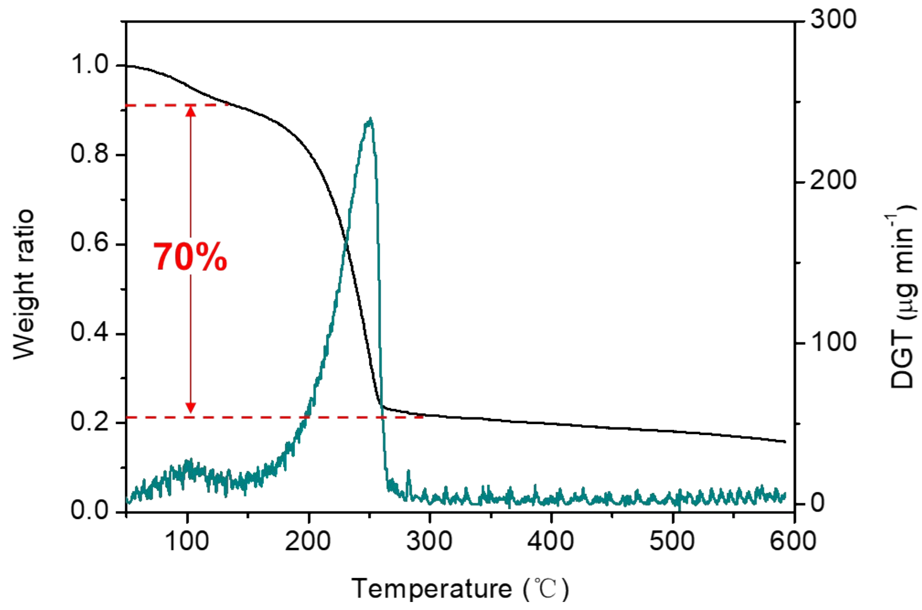

Figure S12. TGA and DTG profiles of S@HPCK containing ~70 wt.% S in N_2 atomsphere.

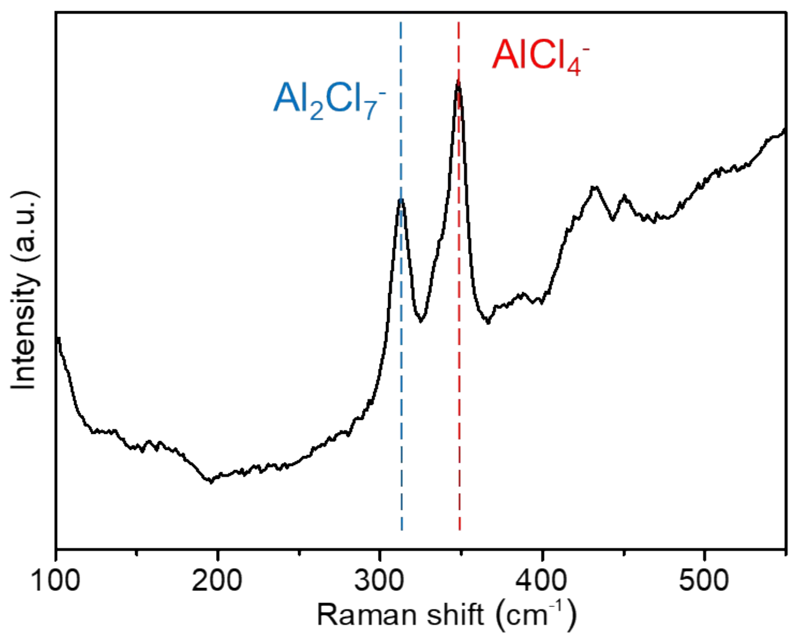

Figure S13. Raman spectrum of $AlCl_3$-AcA (1.3:1 in molar ratio) electrolyte.

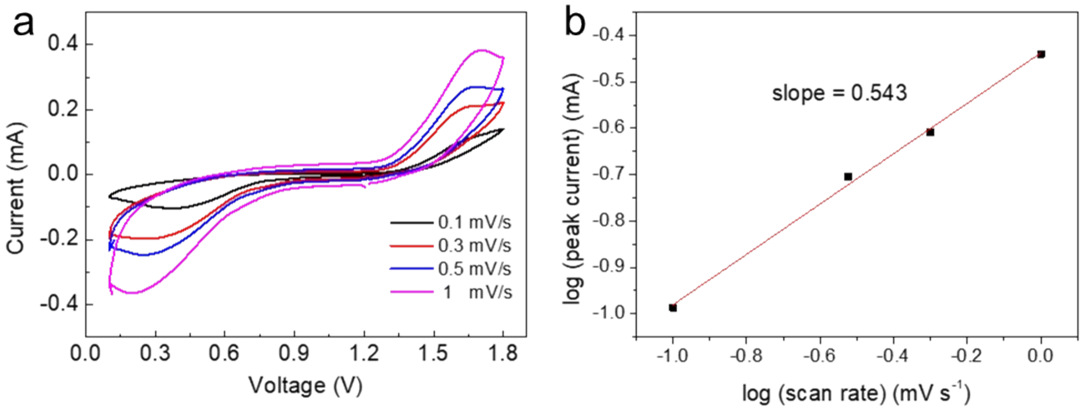

Figure S14. (a) CV profiles of S@HPCK under different scan rate. (b) Linear stimulation of the plot of current of the discharge peak *vs.* the scan rate.

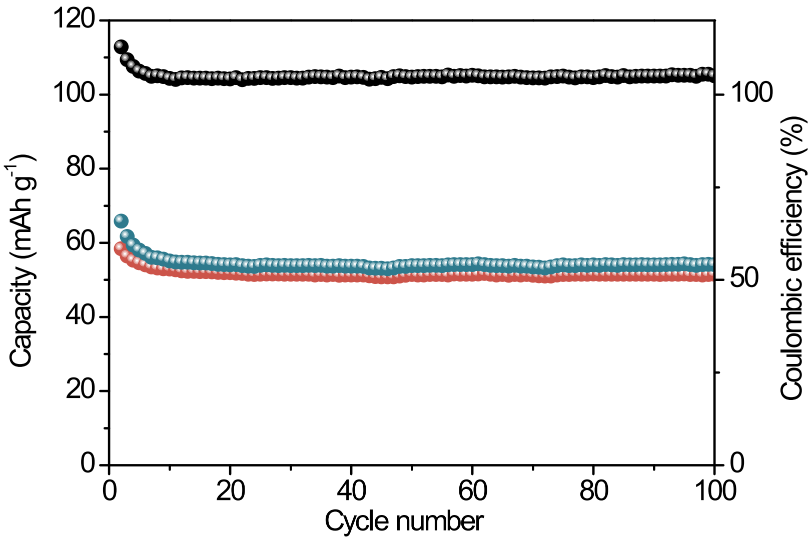

Figure S15. Cycle performance of an Al-HPCK battery at 0.2 A g^{-1}.

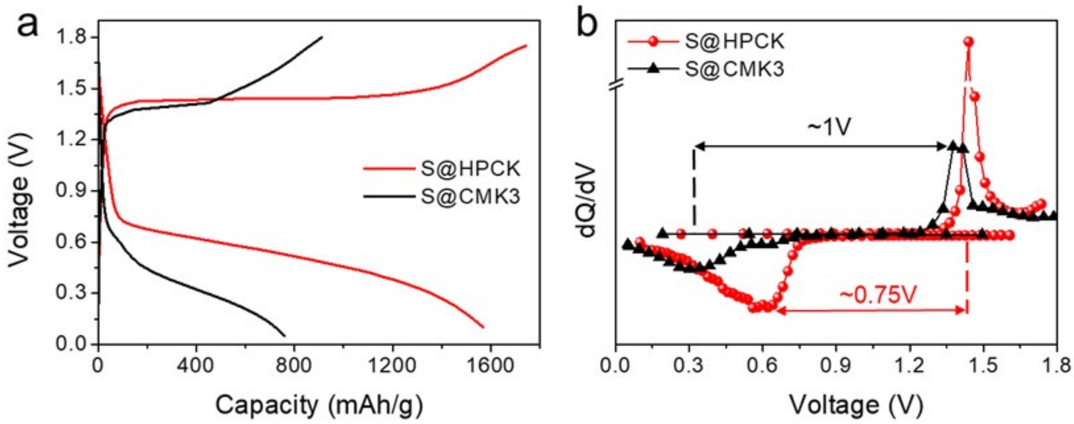

Figure S16. A comparison of the voltage hysteresis between the S@HPCK- and S@CMK3-based Al-S batteries. (a) The representative charge/discharge curves of the two batteries at 0.2 A g^{-1}. (b) The corresponding dQ/dV curves of the charge/discharge curves in (a).

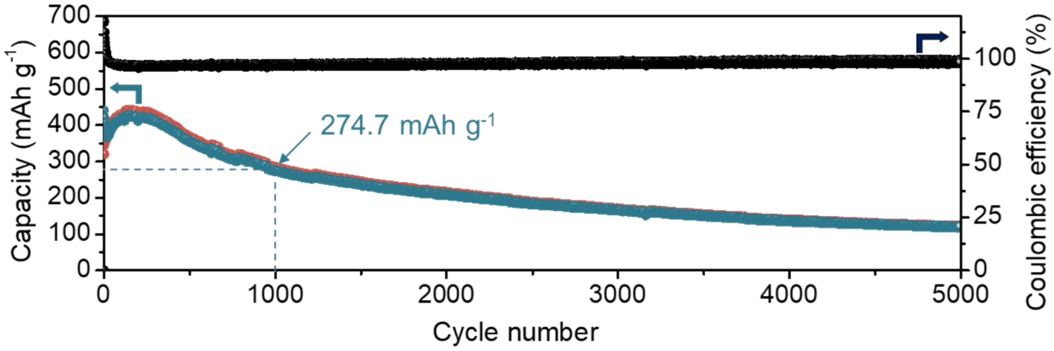

Figure S17. Long-cycle performance of the Al-S@ HPCK battery at 2 A g^{-1}.

Figure S18. Soft-pack batteries (five batteries in series) for lighting up a set of LED lights.

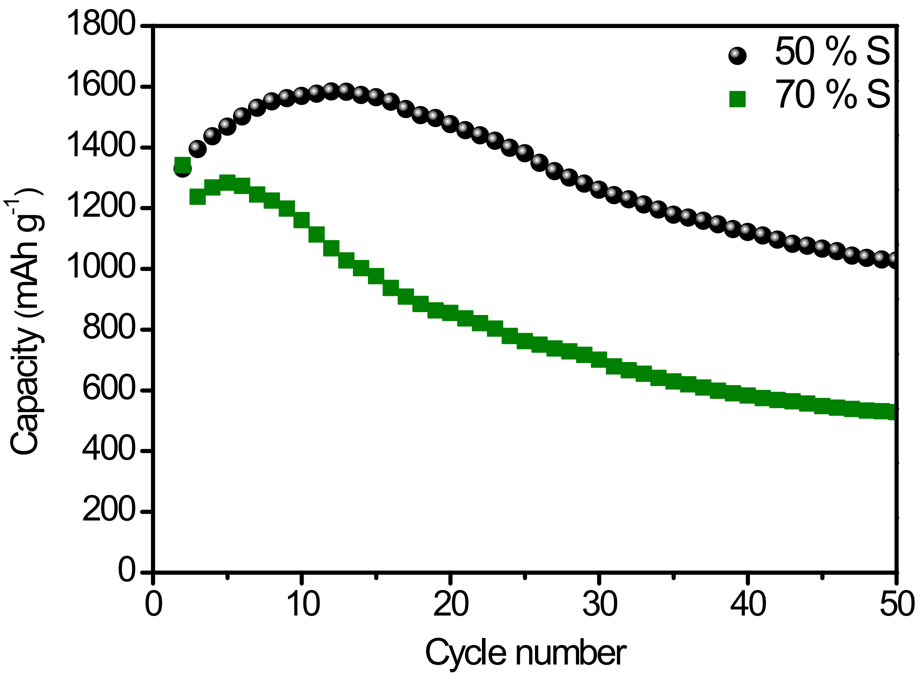

Figure S19. Cycling performance of Al-S@HPCK battery at 0.2 A g^{-1} using S@HPCK cathodes containing 50 wt.% and 70 wt. % S.

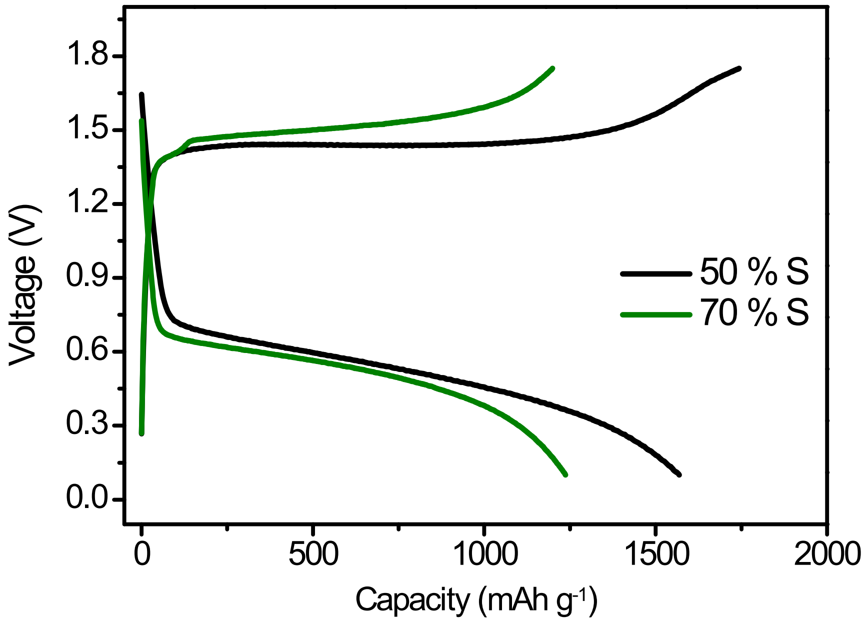

Figure S20. The representative galvanostatic charge/discharge curves of S@HPCKs with 50 wt.% and 70 wt. % S.

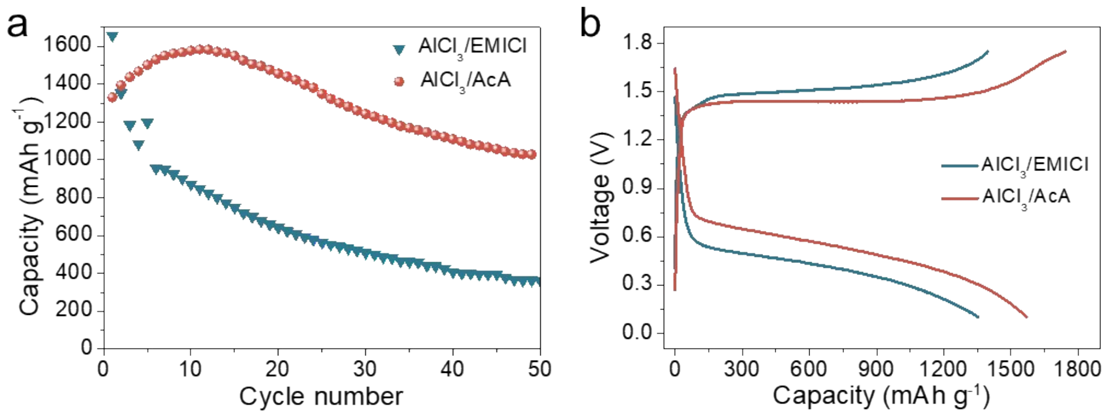

Figure S21. The performances of Al-S@HPCK batteries using $AlCl_3$/AcA and $AlCl_3$/EMICl as the electrolyte. (a) The cycle performances at a current density of 0.2 A g^{-1}, and (b) the typical galvanostatic charge/discharge curves.

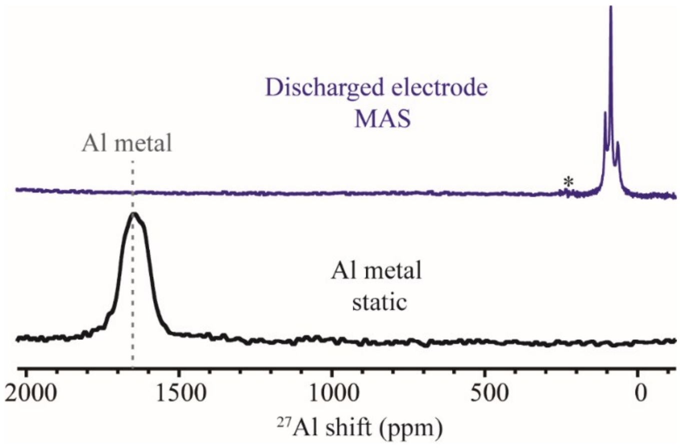

Figure S22. ^{27}Al NMR spectra of the discharged electrode obtained under MAS and the pure Al metal measured under static conditions. The peak marked with asterisk is the spinning sideband (SSBs).

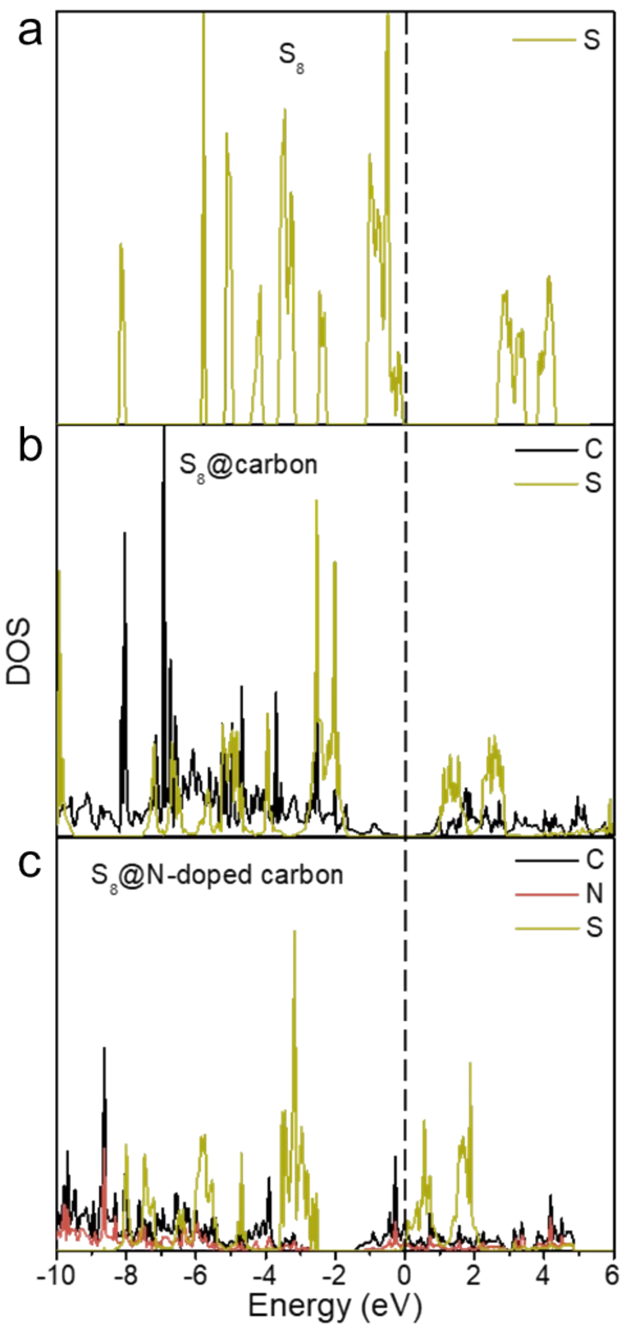

Figure S23. Densities of states for (a) sulfur, (b) the composite of sulfur loaded by carbon and (c) the composite of sulfur loaded by N-doped carbon.

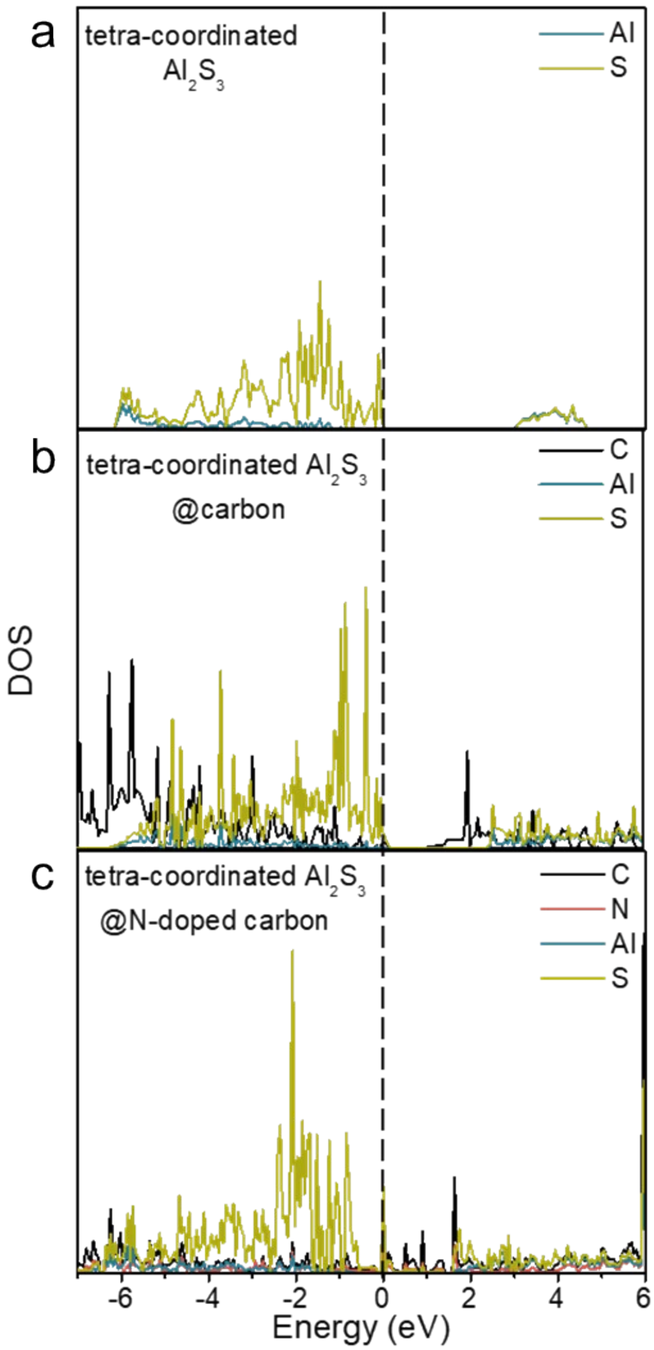

Figure S24. Densities of states for (a) tetra-coordinated Al_2S_3, (b) the composite of tetra-coordinated Al_2S_3 loaded by carbon and (c) the composite of tetra-coordinated Al_2S_3 loaded by N-doped carbon.

Table S1. Performances of recently works for Al-S batteries. Note some values were calculated from the provided figures in the references.

Cathode	Capacity -current density-cycle number	Voltage hysterisis	S content	Capacity retention-cycle number	Coulombic efficiency
S@ Ketjen black@PVDF[1]	1600 mAh g^{-1} – 20 mA g^{-1} – 1^{st} 1200 mAh g^{-1} – 120 mA g^{-1} – 1^{st}	~ 0.75 V	50%	not reported	not reported
Activated carbon cloth/sulfur composite[2]	1320 mAh g^{-1} – 50 mA g^{-1} – 1^{st} 1000 mAh g^{-1} – 50 mA g^{-1} – 20^{th}	~ 0.78 V	1 mg cm^{-2}	75.8% - 20^{th}	not reported
S@CMK-3[3]	1390 mAh g^{-1} – 251 mA g^{-1} – 1^{st} >400 mAh g^{-1} – 251 mA g^{-1} – 20^{th}	~ 0.75 V	40%	>30.8% - 20^{th}	not reported
S dispersion of sulfur-ionic liquid slurry into an activated CNF paper[4]	>1200 mAh g^{-1} – C/20 – 1^{st} >550 mAh g^{-1} – C/20 – 10^{th}	~ 0.8V	not reported	45.8% - 10^{th}	not reported
S dispersion of sulfur-ionic liquid slurry into an activated CNF paper[5]	~1000 mAh g^{-1} – C/20 – 1^{st} ~600 mAh g^{-1} – C/20 – 50^{th}	~ 0.75 V	not reported	~60% - 50^{th}	~90% - 50^{th}
S@CMK-3[6]	2100 mAh g^{-1} – 100 mA g^{-1} – 1^{st} >500 mAh g^{-1} – 100 mA g^{-1} – 60^{th}	~ 0.8 V	50%	>23.8% - 60^{th}	84.9% - 20^{th}

S@HKUST-1-C[7]	>1000 mAh g^{-1} – 1 A g^{-1} – 1st 460 mAh g^{-1} – 1 A g^{-1} – 500th	~ 1 V	34.3%	46% - 500th	95% - 500th at 1A g^{-1}
S@Co/C[8]	500 mAh g^{-1} – 1 A g^{-1} – 200th	~0.7 V	50%	30% - 200th	~90% - 200th at 1 A g^{-1}
This work	1330 mAh g^{-1} – 0.2 A g^{-1} – 1st 1027 mAh g^{-1} – 0.2 A g^{-1} – 50th	~0.7 V	50%	77.2% - 50th at 0.2 A g^{-1}	90.8% - 50th at 0.2 A g^{-1}
	829 mAh g^{-1} – 1 A g^{-1} – 1st 405 mAh g^{-1} – 1 A g^{-1} – 700th		70%	48.9% - 700th at 1 A g^{-1}	96.2% - 700th at 1 A g^{-1}

References

[1] G. Cohn, L. Ma, L. A. Archer. *J. Power Sources* 283 (2015) 416-422.

[2] T. Gao, X. Li, X. Wang, J. Hu, F. Han, X. Fan, L. Suo, A. J. Pearse, S. B. Lee, G. W. Rubloff, K. J. Gaskell, M. Noked, C. Wang. *Angew. Chem. Int. Ed.* 55 (2016) 9898-9901.

[3] H. Yang, L. Yin, J. Liang, Z. Sun, Y. Wang, H. Li, K. He, L. Ma, Z. Peng, S. Qiu, C. Sun, H. M. Cheng, F. Li. *Angew. Chem. Int. Ed.* 57 (2018) 1898-1902.

[4] X. Yu, A. Manthiram. *Adv. Energy Mater.* 7 (2017) 1700561.

[5] X. Yu, M. J. Boyer, G. S. Hwang, A. Manthiram. *Chem.* 4 (2018) 586-598.

[6] W. Chu, X. Zhang, J. Wang, S. Zhao, S. Liu, H. Yu. *Energy Storage Mater.* 22 (2019) 418-423.

[7] Y. Guo, H. Jin, Z. Qi, Z. Hu, H. Ji, L.-J. Wan. *Adv. Funct. Mater.* 29 (2019) 1807676.

[8] Y. Guo, Z. Hu, J. Wang, Z. Peng, J. Zhu, H. Ji, L. J. Wan. *Angewandte Chemie International Edition* (2020).